Study of the Magnetocaloric Effect by Means of Theoretical Models in La0.6Ca0.2Na0.2MnO3 Manganite Compound

Bandar Alzahrani, Mohamed Hsini, Sobhi Hcini, Michel Boudard, Abdessalem Dhahri, Mohamed Lamjed Bouazizi

Study of the magnetocaloric effect by means of theoretical models in $La_{0.6}Ca_{0.2}Na_{0.2}MnO_3$ manganite compound

Bandar Alzahrani[1], Mohamed Hsini[2], Sobhi Hcini[3], Michel Boudard[4], Abdessalem Dhahri[2,] *, Mohmed Lamjed Bouazizi[1]

[1] *Prince Sattam Bin Abdulaziz University, College of Engineering, Al Kharj, Kingdom of Saudi Arabia.*
[2] *University of Monastir, Faculty of Science of Monastir, Laboratory of Physical Chemistry of Materials, Department of Physics, Monastir 5019, Tunisia.*
[3] *University of Kairouan, Faculty of Science and Technology of Sidi Bouzid, Research unit of valorization and optimization of exploitation of resources, 9100 Sidi Bouzid, Tunisia.*
[4] *University of Grenoble Alpes, LMGP, CNRS, 38000 Grenoble, France.*

* Corresponding authors: E-mail address: ba.alzahrani@psau.edu.sa, dh.abdessalem@gmail.com

Abstract

In this work, an overview of the Weiss molecular mean-field theory, the Bean-Rodbell model, and the Landau theory is presented, providing the theoretical background for simulating the magnetocaloric properties for $La_{0.6}Ca_{0.2}Na_{0.2}MnO_3$ manganite. Results showed that sample exhibits second order ferromagnetic (FM) – paramagnetic (PM) magnetic phase transition and relatively higher values of magnetic entropy change ($-\Delta S_M$). In application point of view, this material can be used in magnetic refrigeration technology. The theoretical values of $-\Delta S_M$ determined using each theory agree well with the experimental ones estimated from Maxwell relations. In other part, a good agreement in the spontaneous magnetization values, $M_{spont}(T)$, estimated from ($-\Delta S_M$ vs. M^2) and (H/M vs. M^2) data was found. Also, the values of the critical exponent (β) found from both methods are close and check that the mean field model is adequate to study the MCE in $La_{0.6}Ca_{0.2}Na_{0.2}MnO_3$ sample.

Keywords: Manganites; Magnetocaloric effect; Theoretical models; Spontaneous magnetization.

1. Introduction

The current refrigeration machines are based on the well known and well mastered conventional principle of compression/expansion of gas. But this universally widespread technology generates significant CO_2 emissions and involves leaks of refrigerants such as CFCs (chlorofluorocarbons) and HCFCs (hydrochlorofluorocarbons) contributing to the destruction of the ozone layer and to the greenhouse effect in general [1]. In reality, traditional refrigeration production has reached its limits in the context where refrigerant gases are subject to environmental restrictions, and today the need to find new, less polluting refrigeration systems is therefore becoming priority. Research in this area is therefore exploring new technics. One of the most promising alternatives is the magnetic refrigeration; an emerging technology that uses compact systems (solid and non-volatile materials as active components), quiet, clean and energy efficient [2-7]. This technology, credible for producing "ecological" and energy efficient cooling, is based on the magnetocaloric effect (MCE) presented by certain magnetic materials. During the last years, numerous prototypes of magnetic refrigeration have been produced, but there is still progress to be made both at the fundamental and practical levels to make this technology industrializable and commercially competitive compared to the conventional refrigeration.

As a result, current research has mainly turned to several families of ferromagnetic materials having giant MCE. Manganites having general formula of $Ln_{1-x}M_xMnO_3$ (Ln and M are rare earth element and alkaline earth ion, respectively) represent one of the studied families due to their remarkable MCE [8-16]. Among manganite systems, the parent $La_{0.8}Ca_{0.2}MnO_3$ compound is one of the extensively studied manganite in the literature. This sample possesses a Curie temperature (T_C) relatively lower than room temperature [17-20] which limits the possibility of its applications in the magnetic refrigeration field. This motivated us, in this work, to seek improvements in the magnetocaloric properties of the

$La_{0.8}Ca_{0.2}MnO_3$ compound. Based on some previous works, we have observed that the substitution of the rare earth (La) by a monovalent cation such as Na leads to the increase of the Curie temperature of La-based manganites (see [1] for a review). Therefore, the Curie temperature for $La_{0.8}Ca_{0.2}MnO_3$ sample can be adjusted to the room temperature by partial replacement of La^{3+} by Na^{+}. Consequently, we have presented in this work a manganite system having $La_{0.6}Ca_{0.2}Na_{0.2}MnO_3$ as composition.

In a previous work [21], we have investigated the structural, magnetic, critical and magnetocaloric properties of $La_{0.6}Ca_{0.2}Na_{0.2}MnO_3$ manganite. The main experimental results of this study are:

i) The sample crystallizes in the rhombohedral structure with $R\bar{3}c$ space group.

ii) The sample undergoes a second order FM – PM magnetic phase transition around its Curie temperature T_C = 275 K.

iii) The magnetic entropy change ($-\Delta S_M$) estimated from maxwell relation and the relative cooling power (RCP) are relatively higher making the sample promising candidate for the magnetic refrigeration technology.

iv) The estimated critical exponents are in good agreement with the mean-field model.

However, the optimization and development of magnetic refrigeration materials requires an in-depth thermodynamic description. In this case, significant progress has been made in the interpretation of magnetocaloric properties of materials. The overview on the mean-field theory provides us with the basic theoretical notions to simulate the magnetic and magnetocaloric properties of manganite materials. The thermodynamics of the mean-field model presents an efficient method for estimating the MCE from experimental data of magnetic isotherms. The generalized formulation of the molecular interaction according to the mean-field leads to a scaling method [22-24], which allows the direct estimation of several magnetic parameters from experimental data. The Weiss molecular mean-field theory

combined to the Bean-Rodbell model [25, 26], also allow to adequately simulate the magnetic and magnetocaloric properties and to verify the type of FM-PM phase transition of the magnetic system. In addition, the Landau's theory is able to study the MCE in ferromagnetic systems with magneto-elastic and magneto-electronic couplings [27-30]. Also, the study of critical phenomena shows an universal magnetocaloric behavior in materials with second-order magnetic phase transitions (SOMPT) [31, 32].

Our study in this work falls within this context. The molecular mean-field theory, Bean-Rodbell model and Landau theory are exploited to study the MCE in $La_{0.6}Ca_{0.2}Na_{0.2}MnO_3$ manganite. The theoretical values of magnetic entropy change and spontaneous magnetization are compared to those determined experimentally.

2. Experimental

To prepare $La_{0.6}Ca_{0.2}Na_{0.2}MnO_3$ manganite, we have used the sol-gel method. The different precursors used for the production of this sample are the lanthanum, calcium, sodium and manganese nitrates. These nitrates were weighed in stoichiometric quantities and then dissolved in distilled water with thermal stirring at 90 ° C to obtain mixed solution. Following this step, we have added into the solution the citric acid as complexing agent for the different cations. Subsequently, the pH of the solution was adjusted to around 7 by adding the ammonia. After this step, we have added the ethylene glycol which has been used as a polymerization agent. After approximately 4 h, the formation of a viscous liquid (gel) is observed, which was subsequently dried in an oven at 200 °C (for 6 h). The resulting precursor was ground and the obtained powder was undergone a few cycles of grinding, pelleting and sintering. Finally, the structure of the sample was well formed at 1100 °C (for 24 h).

The *M(H, T)* isotherm measurements were performed using BS1 and BS2 linear extraction magnetometers near the Curie temperature (T_C) as a function of magnetic field and temperature in 0 T ≤ H ≤ 5 T and 235 K ≤ T ≤ 320 K intervals, respectively.

3. Results and discussion

Fig. 1a shows isotherms *M(H, T)* taken near T_C= 275 K for $La_{0.6}Ca_{0.2}Na_{0.2}MnO_3$ manganite. From this experimental data, the variation of $-\Delta S_M$ is given according to the following Maxwell relations as follows [1]:

$$\left(\frac{\partial S}{\partial H}\right)_T = \left(\frac{\partial M}{\partial T}\right)_H \quad (1)$$

$$\left(\frac{\partial S}{\partial M}\right)_T = -\left(\frac{\partial H}{\partial T}\right)_M \quad (2)$$

Using Eq. (1), the $-\Delta S_M$ values can be estimated from the *M (H, T)* data as:

$$-\Delta S_M(T, \Delta H) = -\int_0^H \left(\frac{\partial M}{\partial T}\right)_H dH \quad (3)$$

Using the isotherms *M(H, T)*, the $-\Delta S_M(T, H)$ curves are estimated using Eq. (3) and presented in Fig. 1b. The curves show peaks defined as maximum entropy change (ΔS_M^{max}) around T_C. At applied magnetic field of 5 T, the ΔS_M^{max} reachs value of about 3.09 $Jkg^{-1}\ K^{-1}$.

For a ferromagnetic material, the magnetization (M) is linked to the applied magnetic field H, the temperature T and the exchange field H_{exch}= λM (here λ is the mean-field exchange parameter). Also, it can be modeled by the Brillouin function $B_J(x)$ as [33]:

$$M = f\left(\frac{H+H_{exch}}{T}\right) = M_0 B_J(x) \quad (4)$$

where M_0 = saturation magnetization, and $B_J(x)$ can be expressed as:

$$B_J(x) = \frac{2J+1}{2J}\coth\left(\frac{2J+1}{2J}x\right) - \frac{1}{2J}\coth\left(\frac{x}{2J}\right) \text{ with } x = \frac{Jg\mu_B}{k_B}\left(\frac{H+H_{exch}}{T}\right) \quad (5)$$

Here g, J, μ_B and k_B are the gyromagnetic factor, the spin momentum, the Bohr magneton and the Boltzmann constant respectively. By applying the reciprocal function f^{-1} of f on the first member of Eq. (4), we may get:

$$\frac{H}{T} = f^{-1}(M) - \frac{H_{exch}}{T} = f^{-1}(M) - \frac{\lambda M}{T}. \quad (6)$$

In order to determine the dependence of H_{exch} on M, Fig. 1a was analysed to follow the variation of $\frac{H}{T}$ vs. $\frac{1}{T}$ at constant magnetization values (M= 2.5 emu.g^{-1} by step) as depicted in Fig. 2a. Then, to obtain the H_{exch} values, each curve was adjusted by a linear adjustment (red lines in Fig. 2a) according to Eq. (6). The H_{exch} parameter is defined as the slope of each curve. Fig. 2b indicates the H_{exch} vs. M curve fitted by $H_{exch} = \lambda_1 M + \lambda_3 M^3$ equation [34, 35]. This adjustment shows negligible value of λ_3 parameter ($\lambda_3 = -0.0003$ (Temu^{-1}g)^3), so H_{exch} is approximately as $H_{exch} = \lambda_1 M \approx \lambda M$, with $\lambda_1 = 1.37$ T emu^{-1}g. Then, the building of scaling plot of M vs.$\frac{H+H_{exch}}{T}$ is showed in Fig. 3 (black symbols). From Fig. 3, we noted the overlay of all the curves along one curve. Using Eq. (4), the fit of these curves leads to the determination of the experimental values of J, g and M_0 parameters which are found respectively as 2.02, 1.98 and 55.2 emu.g^{-1}. Based on the Hund rules and taking into account that orbital momentum is quenched for transition metals [36], only the contributions of Mn^{3+} and Mn^{4+} take place in $La^{3+}_{0.6}Ca^{2+}_{0.2}Na^{2+}_{0.2}Mn^{3+}_{0.2}Mn^{4+}_{0.8}O^{2-}_3$ system, giving $J = g = 2$. A good agreement between the theoretical and adjusted values is clearly observed. The adjusted values of λ, J, g and M_0 are reinjected in Eq. (4) to generate the *M(H)* curves (red lines), which are correlated well with the experimental curves (black symbols) as shown in Fig. 4a. On the other hand, from the Bean-Rodbell model the reduced magnetization σ is linked to to the brillouin function as [37, 38]:

$$\sigma(Y) = B_J(Y), \quad (7)$$

with $Y = \frac{1}{T}\left[3T_0\left(\frac{J}{J+1}\right)\sigma + \frac{gJ\mu_B}{k_B}H + \frac{9}{5}\frac{(2J+1)^4-1}{[2(J+1)]^4}T_0\eta\sigma^3\right]$, T_0 is the Curie temperature if the magnetic interactions are considered and η is a parameter that checks the order of magnetic phase transitions. The first order magnetic phase transition occurs if $\eta > 1$, while the SOMPT arises if $\eta < 1$. By replacing x in Eq. (4) by Y (see Eq. (7)), the generated *M(T)* curves (red

lines) match well with the experimental ones (black symbols) as indicated in Fig. 4b for $\eta = 0.08$ and T_0 = 275 K. Since $\eta < 1$, the SOMPT is checked. Eqs. (7) and (2) lead to the estimation of $-\Delta S_M$ as:

$$-\Delta S_M(T)_{H_1 \to H_2} = \int_{M|_{H_1}}^{M|_{H_2}} \left(f^{-1}(M) - \left(\frac{\partial \lambda(T)}{\partial T}\right)_M M \right) dM. \quad (8)$$

The resolution of Eq. (8) is achieved with the *Mean-Field Simulation software*. This allows us to set the evolution of $-\Delta S_M$ vs. T curves under various ΔH as represented in Fig. 5.

To model the magnetic entropy change, described by the spin fluctuations, we have expanded the development of the Landau free energy, including the magnetic energy MH, to the eighth order as in our previous work [39]:

$$F(T,M) \cong F_0 + \frac{1}{2}A(T)M^2 + \frac{1}{4}B(T)M^4 + \frac{1}{6}C(T)M^6 + \frac{1}{8}D(T)M^8 + \cdots - MH, \quad (9)$$

here the Landau coefficients $A(T)$, $B(T)$, $C(T)$ and $D(T)$ are temperature-dependent parameters which represent the magnetoelastic coupling and electrons interaction [40]. At T_C and from the equilibrium condition, $\frac{\partial \mathrm{F}}{\partial \mathrm{M}} = 0$, the magnetic equation state obtained from Eq. (9), is given as:

$$\frac{H}{M} = A(T) + B(T)M^2 + C(T)M^4 + D(T)M^6. \quad (10)$$

The Landau coefficients are determined from the polynominal fit of Arrott plots $\left(\frac{\mathrm{H}}{\mathrm{M}}\ vs.\ \mathrm{M}^2\right)$ using Eq. (10) as shown in Fig. 6a. The evolution of *A*, *B*, *C*, and *D* coefficients are shown in Fig. 6b and c as a function of temperature. The results cleary indicate that $A(T)$ has a positive sign with a minimum around T_C and $B(T_C)$ is positive confirming the SOMPT for the $La_{0.6}Ca_{0.2}Na_{0.2}MnO_3$ sample. In other hand, the differentiation of the Landau free energy in Eq. (9) allows us to estimate the $-\Delta S_M(T)$ variation as:

$$-\Delta S_M(T) = -\left(\frac{\partial F(M,T)}{\partial T}\right)_M = \frac{1}{2}A'M^2 + \frac{1}{4}B'M^4 + \frac{1}{6}C'M^6 + \frac{1}{8}D'M^8\ , \quad (11)$$

where $A' = \frac{\partial A}{\partial T}$, $B' = \frac{\partial B}{\partial T}$, $C' = \frac{\partial C}{\partial T}$ and $D' = \frac{\partial D}{\partial T}$. After deriving *A*, *B*, C and *D* parameters, the temperature dependence of $(-\Delta S_M)$ under various ΔH is estimated from Eq. (11) and plotted in Fig. 7. The estimated ($-\Delta S_M$ vs. T) curves under ΔH varying from 0 to 5 T, from the the molecular mean-field theory (Fig. 5) and the Landau theory (Fig. 7) are well compared to those experimentaly estimated using the Maxwell relation (Fig. 1b).

Below T_C, each ferromagnetic material has a spontaneous magnetization, M_{spont}, and consequently the state $\sigma = 0$ is never reached, so it is necessary to add the contribution of the reduced spontaneous magnetization $\sigma_{spont} = \frac{M_{spont}}{M_0}$. So [41, 42],

$$-\Delta S_M(\sigma) = \frac{3J}{J+1} N k_B \left(\sigma^2 + {\sigma_{spont}}^2\right) = \frac{3J}{M_0(J+1)} N k_B \left(M^2 + {M_{spont}}^2\right) \quad (12)$$

To estimate the spontaneous magnetization M_{spont} vs. T for $La_{0.6}Ca_{0.2}Na_{0.2}MnO_3$ sample, the linear parts of Arrott plots $\left(\frac{\mathrm{H}}{\mathrm{M}}\ vs.\ \mathrm{M}^2\right)$ at $T < T_C$ were fitted in Fig. 8a. On the other side, a linear fit serial of the linear regions of $(-\Delta S_M)$ vs. M^2 allows us to determine the values of M_{spont} vs. T as shown in Fig. 8b. An ecxellent agreement between M_{spont} vs. T curves estimated from $\frac{\mathrm{H}}{\mathrm{M}}\ vs.\ \mathrm{M}^2$ (black symbols) and $-\Delta S_M$ vs. M^2 (red symbols) has been found (see Fig. 8c). This result confirms the validity of the magnetic entropy change to estimate the values of the spontaneous magnetization.

The critical exponent β, which describes how the ordered moment grows below T_C, can be estimated from the following relation [43]:

$$M_{spont} \approx log(M_0) + \beta log(-\varepsilon) \quad (13)$$

where $\varepsilon = \frac{T - T_C}{T_C}$ is the reduced temperature. The linear fit of log(M_{spont}) vs $log(-\varepsilon)$ shows that β value calculated when M_{spont} values are estimated from $-\Delta S_M$ vs. M^2 curves is equal to 0.514 (Fig. 9a) and the one deduced when M_{spont} values are estimated from $\frac{\mathrm{H}}{\mathrm{M}}\ vs.\ \mathrm{M}^2$ curves

is equal to 0.510 (Fig. 9b). These two values resulted from these different approximations agree well with the one predicted by the mean field model (β= 0.5).

4. Conclusion

The molecular mean-field, Bean Rodbell and Landau theories, were used successfuly to modeled the $M\ vs.\ H$, M vs. T and $-\Delta S_M$ vs. T curves for $La_{0.6}Ca_{0.2}Na_{0.2}MnO_3$ manganite. The results show good concordance between the theoretical and experimental values. With each model, the second order nature of the FM-PM phase transition has been checked. We have also confirmed the validity of $-\Delta S_M$ to estimate the $M_{spont}(T)$ values. We found that the M_{spont} vs. T curves deduced from $-\Delta S_M$ vs. M^2 agree well with the ones obtained from $\frac{\mathrm{H}}{\mathrm{M}}$ vs. M^2 plots. In addition, we found that the estimated critical exponent (β) for the studied sample is close to that of the mean field model.

Acknowledgements

This work was supported by the Deanship of Scientific Research at Prince Sattam Bin Abdulaziz University under the research Project Number 2017/01/7246.

References

[1] M.H. Phan, S.C. Yu, J. Magn. Magn. Mater. 308 (2007) 325.

[2] N.R. Ram, M. Prakash, U. Naresh, N.S. Kumar, T.S. Sarmash, T. Subbarao, R.J. Kumar, G.R. Kumar, K.C.B. Naidu, J. Supercond. Nov. Magn. 31 (2018) 1971.

[3] V. Franco, J.S. Blázquez, J.J. Ipus, J.Y. Law, L.M. Moreno-Ramírez, A. Conde, Prog. Mat. Science 93 (2018) 112.

[4] N.A. de Oliveira, P.J. von Ranke, Phys. Rep. 489 (2010) 89.

[5] K.A. Gschneidner Jr., V.K. Pecharsky, A.O. Tsokol, Rep. Prog. Phys. 68 (2005) 1479.

[6] E. Brück, J. Phys. D: Appl. Phys. 38 (2005) R381.

[7] J. Lyubina, J. Phys. D: Appl. Phys. 50 (2017) 053002.

[8] K. Riahi, I. Messaoui, W.C. Koubaa, S. Mercone, B. Leridon, M. Koubaa, A. Cheikhrouhou, J. Alloys Compd. 688 (2016) 1028.

[9] H. Ben Khlifa, R. M'nassri, W.C. Koubaa, E.K. Hlil, A. Cheikhrouhou. Ceram. Int. 43 (2017) 8709.

[10] E. Oumezzine, S. Hcini, E.K. Hlil, E. Dhahri, M. Oumezzine, J. Alloys Compd. 615 (2014) 553.

[11] S. Hcini, M. Boudard, S. Zemni, M. Oumezzine, Ceram. Int. 40 (2014) 16041.

[12] S. Mahjoub, M. Baazaoui, E.K. Hlil, M. Oumezzine, Ceram. Int. 41 (2015) 12407.

[13] I. Walha, M. Smari, T. Mnasri, E. Dhahri. J. Magn. Magn. Mater. 454 (2018) 190.

[14] M.R. Laouyenne, M. Baazaoui, Kh. Farah, E.K. Hlil, M. Oumezzine. J. Magn. Magn. Mater. 474 (2019) 393.

[15] M. Zarifi, P. Kameli, T. Raoufi, A. Ghotbi, Varzaneh, D. Salazar, M.I. Nouraddini, L. Kotsedi, M. Maazada, J. Magn. Magn. Mater. 494 (2020) 165734.

[16] A.O. Ayaş, S.K. Çetin, M. Akyol, G. Akça, A. Ekicibil, J. Mol. Struct. 1200 (2020) 127120.

[17] S.O. Manjunatha, A. Rao, V.P.S. Awana, G.S. Okram, J. Magn. Magn. Mater. 394 (2015) 130.

[18] M. Khlifi, M. Bejar, O. EL Sadek, E. Dhahri, M.A. Ahmed, E.H. Hlil, J. Alloys Compd. 509 (2011) 7410.

[19] P.T. Phong, S.J. Jang, B.T. Huy, Y.-I. Lee, I.-J. Lee, J. Mater Sci: Mater Electron 24 (2013) 2292.

[20] Y. Fu, Appl. Phys. Lett. 77 (2000) 118.

[21] N. Mechi, S. Hcini, B. Alzahrani, M. Boudard, A. Dhahri, M.L. Bouazizi, J Supercond Nov Magn (2019) doi:10.1007/s10948-019-05353-9.

[22] M. Hsini, S. Hcini, S. Zemni, J. Magn. Magn. Mater. 466 (2018) 368.

[23] J.S. Amaral, V.S. Amaral, J. Magn. Magn. Mater. 322 (2010) 1552.

[24] M. Hsini, M. Boutaleb, Eur. Phys. J. Plus 135 (2020) 186.

[25] Q. Dong, H. Zhang, J. Sun, B. Shen, V. Franco, J. Appl. Phys. 103 (2008) 116101.

[26] M. Hsini, S. Hcini, S. Zemni, J. Supercond. Nov. Magn. 31 (2018) 81.

[27] V.S. Amaral, J.S. Amaral, J. Magn. Magn. Mater. 272–276 (2004) 2104.

[28] A. Elghoul, A. Krichene, W. Boujelben, J. Phys. Chem. Solids 108 (2017) 52.

[29] H. Yang, Q. Wu, N. Yu, Y. Yu, M. Pan, P. Zhang, H. Ge, J. Solid State Chem. 282 (2020) 121072.

[30] E. Oumezzine, M. Oumezzine, E.K. Hlil J. Alloys Compd. 682 (2016) 366.

[31] S. Hcini, M. Boudard, S. Zemni, M. Oumezzine, Ceram. Int. 41 (2015) 2042.

[32] E. Oumezzine, S. Hcini, E.K. Hlil, E. Dhahri, M. Oumezzine, Physica B 477 (2015) 105.

[33] L. Jia, J. Sun, H. Zhang, F. Hu, C. Dong, B. Shen, J. Phys. Condens. Matter. 18 (2006) 9999.

[34] S. Yahyaoui, M. Khalfaoui, S. Kallel, N. Kallel, J.S. Amaral, A. Ben Lamine, J. Alloys Compd. 685 (2016) 633.

[35] S. Yahyaoui, M. Khalfaoui, S. Kallel, N. Kallel, J.S. Amaral, A. Ben, Lamine, J. Magn. Magn. Mater. 393 (2015) 105.

[36] C. Kittel, Introduction to Solid State Physics, 7th edn. (Wiley, New York, 1996).

[37] A.M. Tishin, Y.I. Spichkin, The Magnetocaloric Effect and its Applications, IOP Publishing, London, 2003.

[38] R. Zach , M. Guillot, J. Tobola, J. Appl. Phys. 83 (1998) 7237.

[39] M. Hsini, S. Hcini, S. Zemni, Eur. Phys. Eur. Phys. J. Plus 134 (2019) 588.

[40] J.S. Amaral, M.S. Reis, V.S. Amaral, T.M. Mendonça, J.P. Araújo, M.A.Sá, P.B. Tavares, J.M. Vieira, J. Magn. Magn. Mater. 290 (2005) 686.

[41] S. Khadhraoui, N. Zaidi, M. Hsini, Z.A. Alrowaili, J. Supercond. Nov. Magn. 32 (2019) 1285.

[42] G.J. Liu, J.R. Sun, J. Lin, Y.W. Xie, T.Y. Zhao, H.W. Zhang, B.G. Shen, Appl. Phys. Lett. 88 (2006) 212505.

[43] H.E. Stanley, Introduction to Phase Transitions and Critical Phenomena, Oxford University Press, London, 1971.

Figures captions

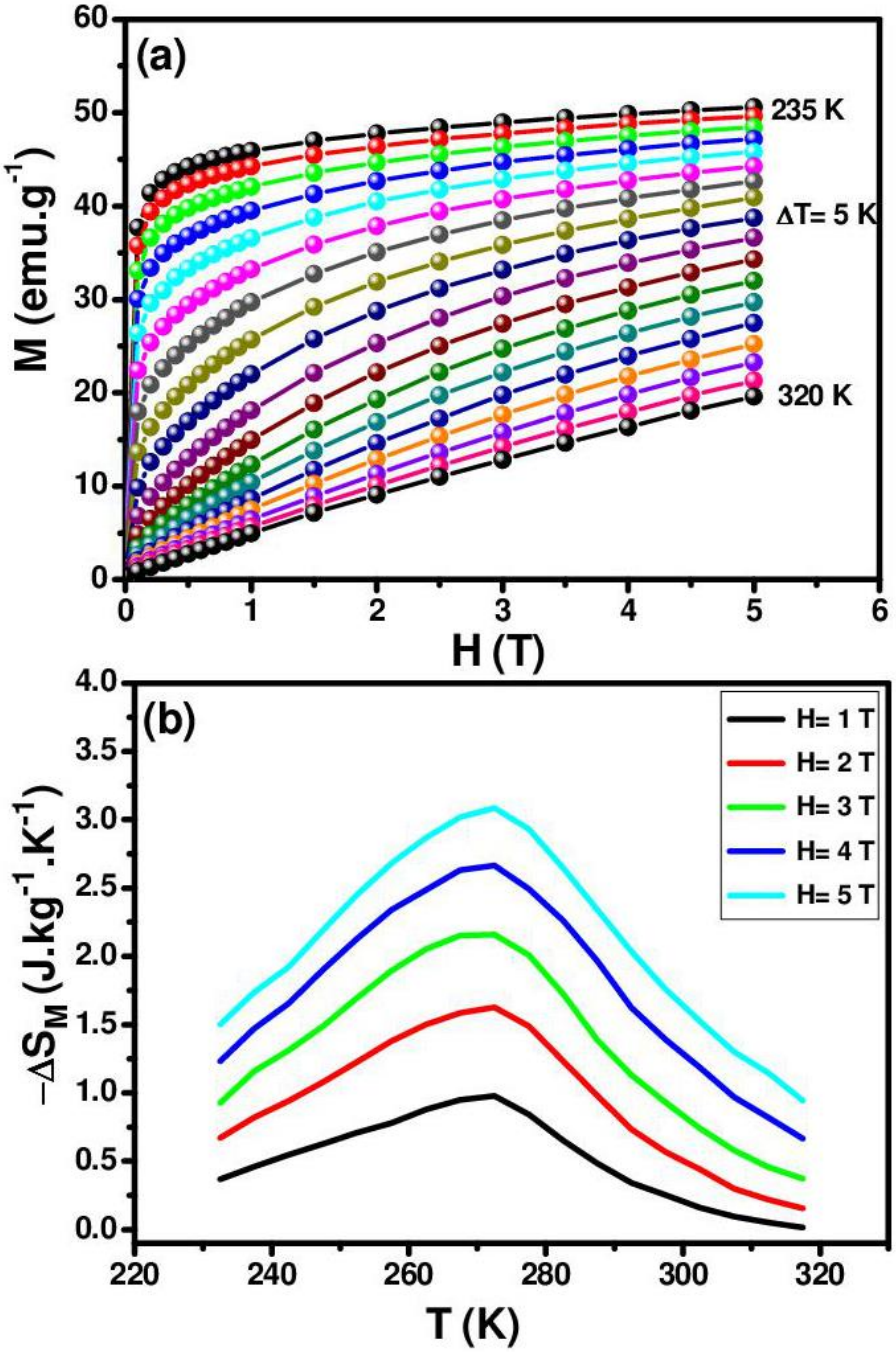

Fig. 1: (a) *M(H, T)* isothermal magnetizations. **(b)** Temperature and applied magnetic fields dependence of the magnetic entropy change estimated from the Maxwell relation.

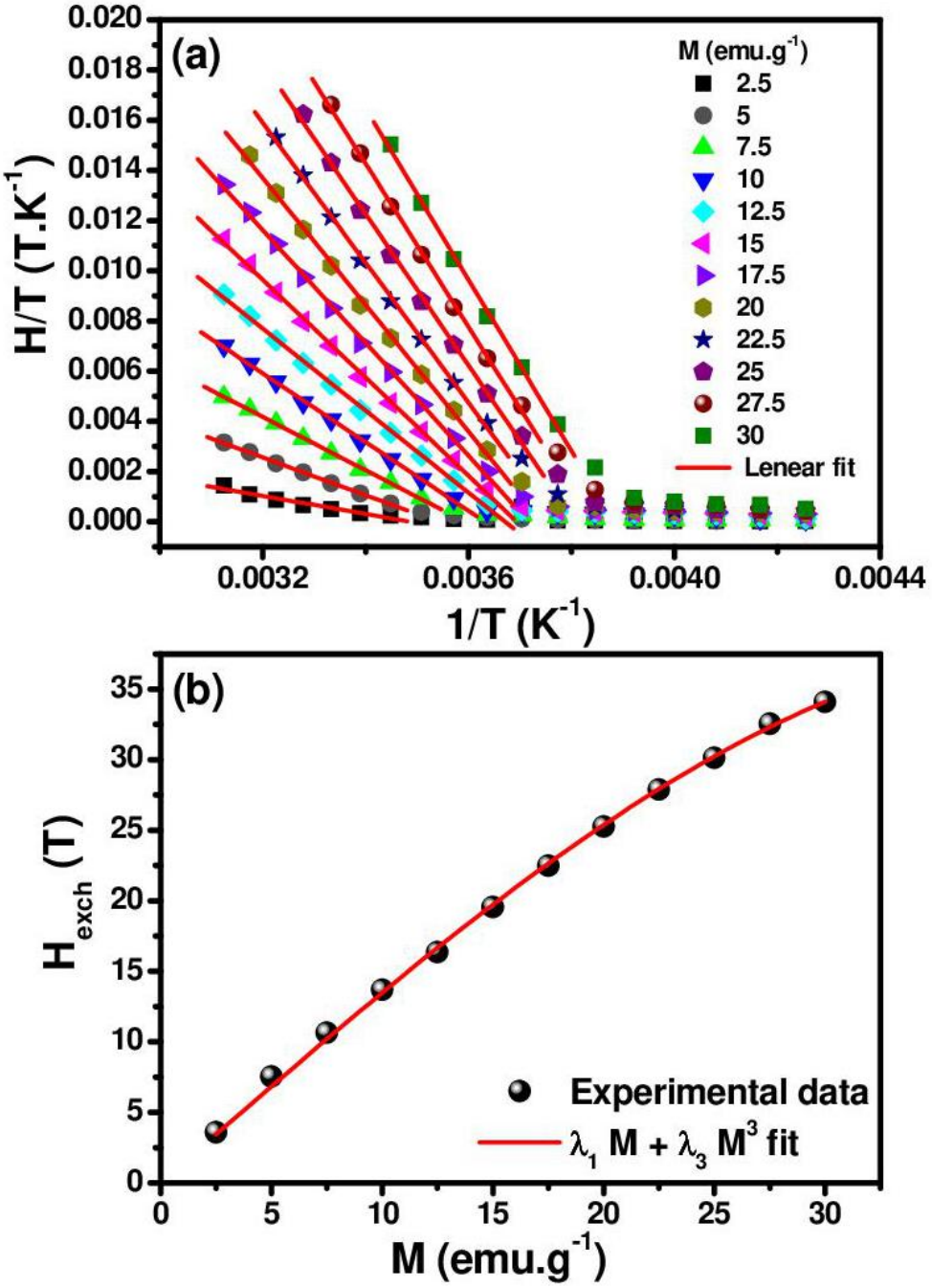

Fig. 2: (a) $\frac{H}{T}$ vs. $\frac{1}{T}$ curves under constant magnetization ($M = 2.5$ emu. g^{-1}). **(b)** H_{exch} vs. M fitted by $\lambda_1 M + \lambda_3 M^3$ function.

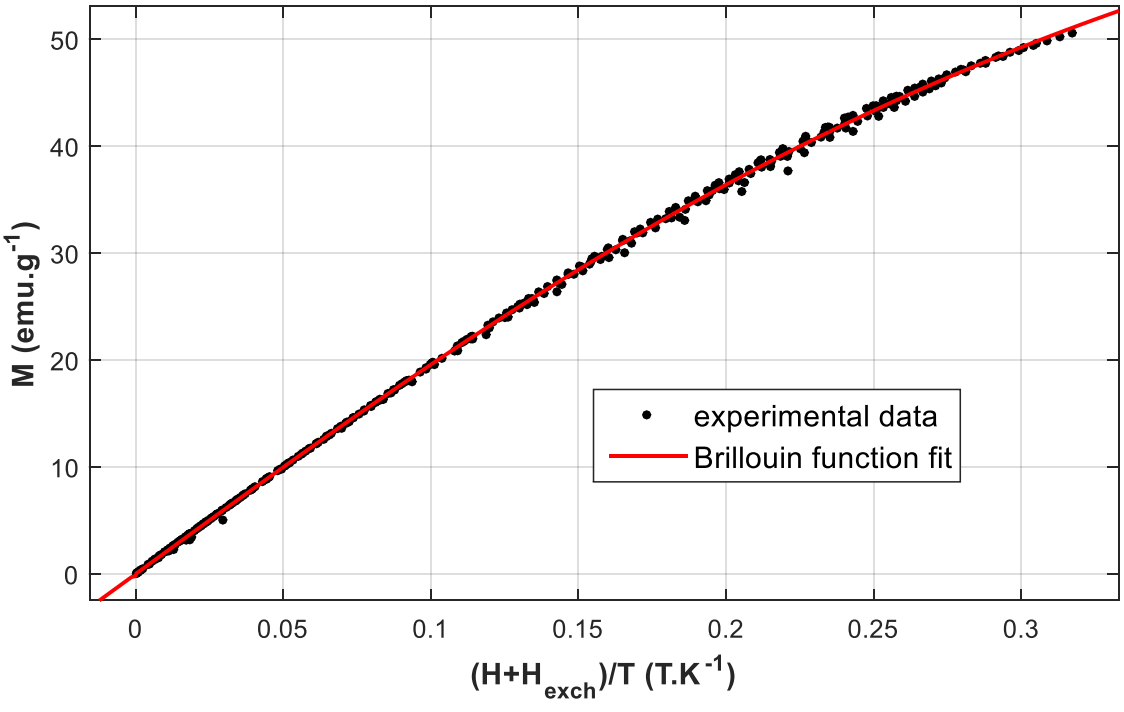

Fig. 3: *M* vs. $\frac{H+H_{exch}}{T}$ scaling plots fitted using Brillouin function.

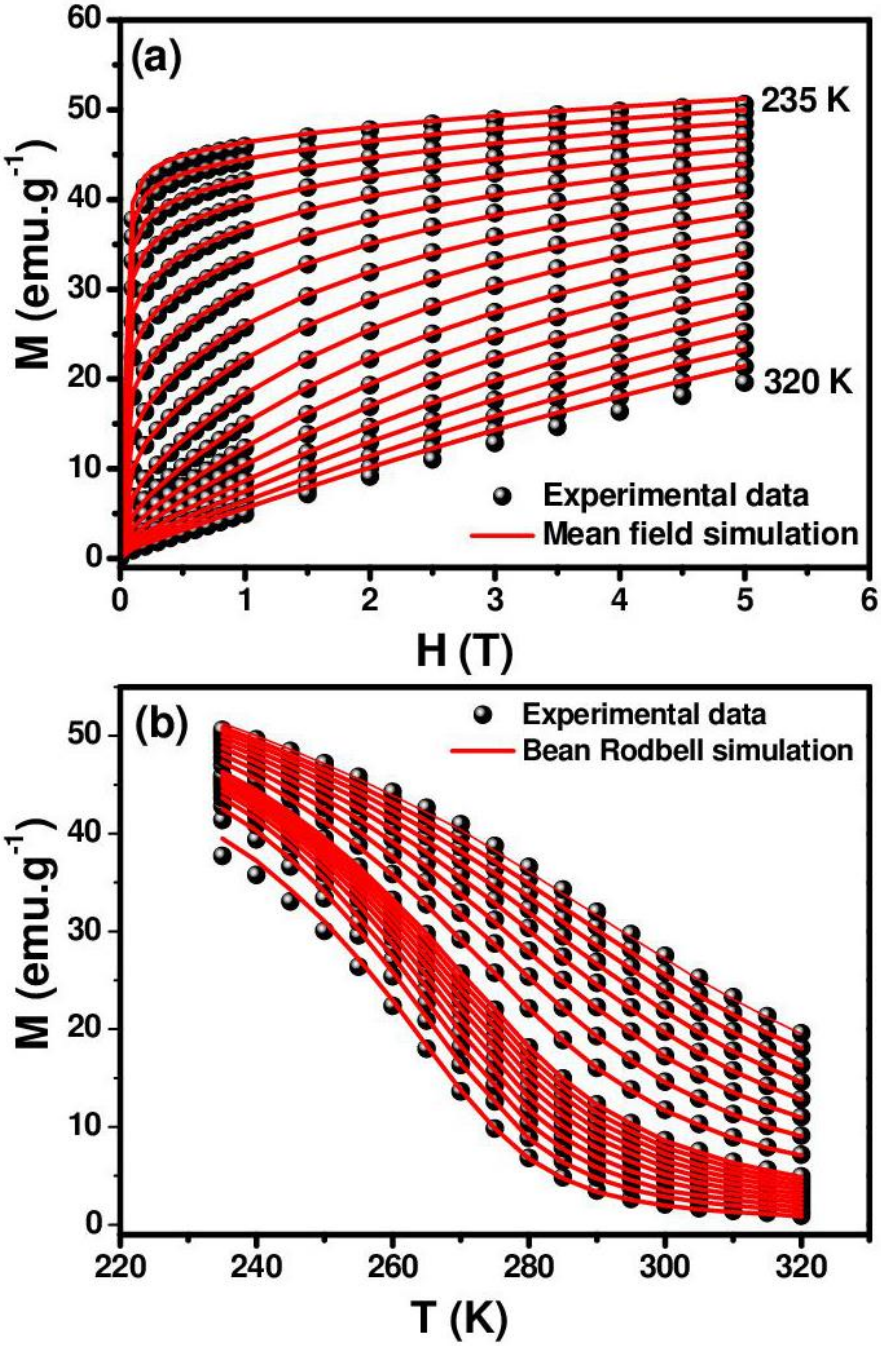

Fig. 4: (a) *M* vs. *H* curves (*black symbols*) with the interpolation using the mean-field method (*red lines*). **(b)** *M* vs. *T* curves (*black symbols*) with the interpolation using the Bean- Rodbell model (*red lines*).

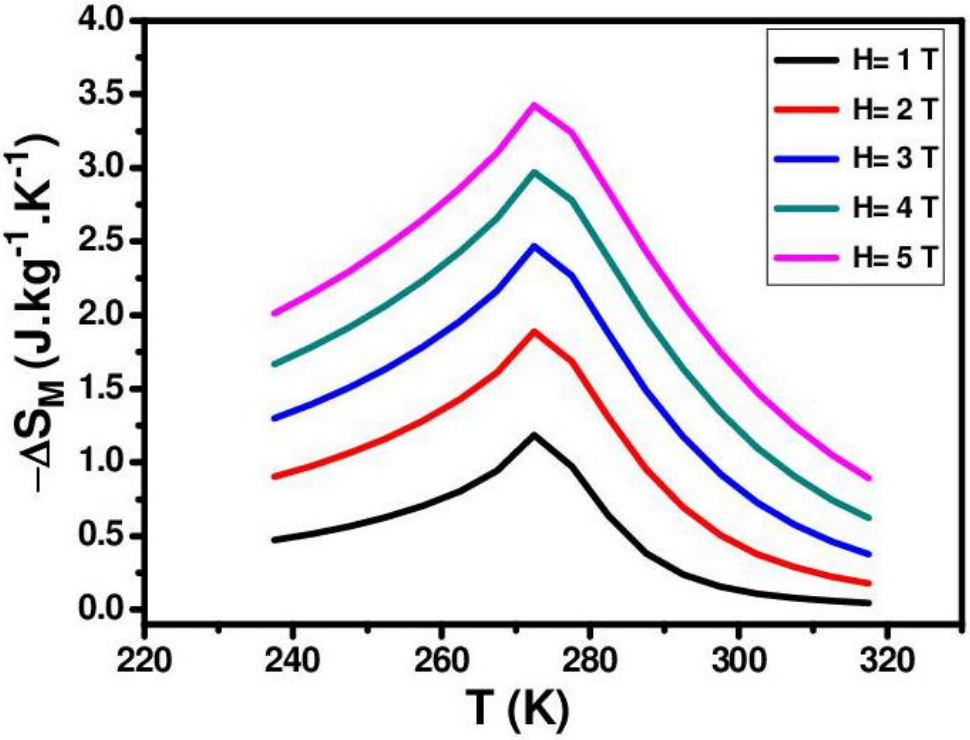

Fig. 5: Temperature and applied magnetic fields dependence of the magnetic entropy change estimated from the molecular mean-field model.

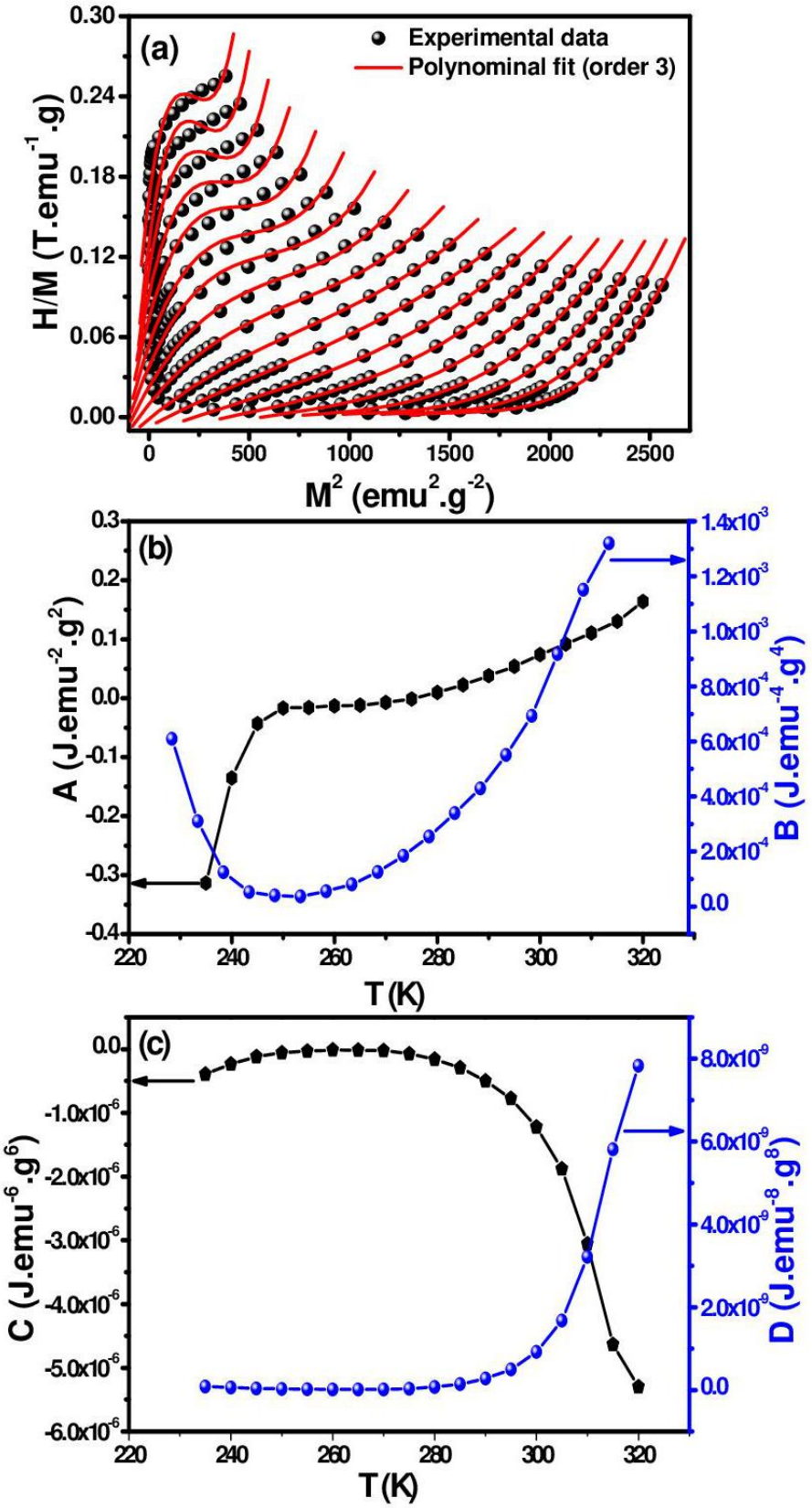

Fig. 6: (a) Quadratic fit (red lines) of $\frac{\mathrm{H}}{\mathrm{M}}$ $vs.\,\mathrm{M}^2$ (black symbols). (**b)** Variations of Landau parameters *A*, *B* vs. *T*. **(c)** Variation of Landau parameters *C* and *D* vs. *T*.

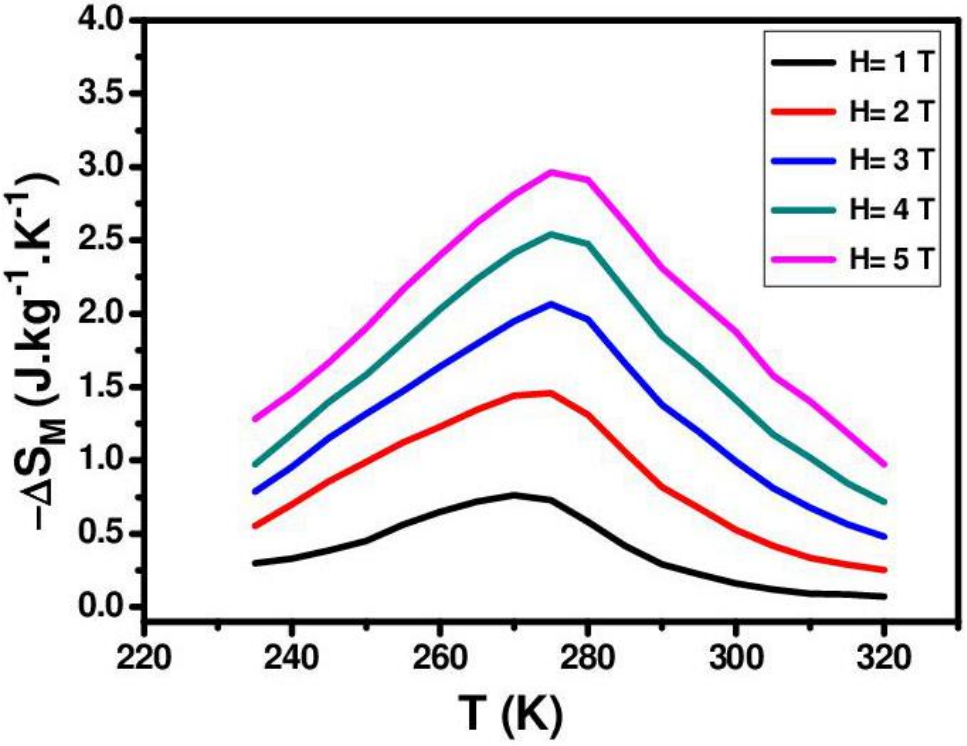

Fig. 7: Temperature and applied magnetic fields dependence of the magnetic entropy change estimated from Landau theory.

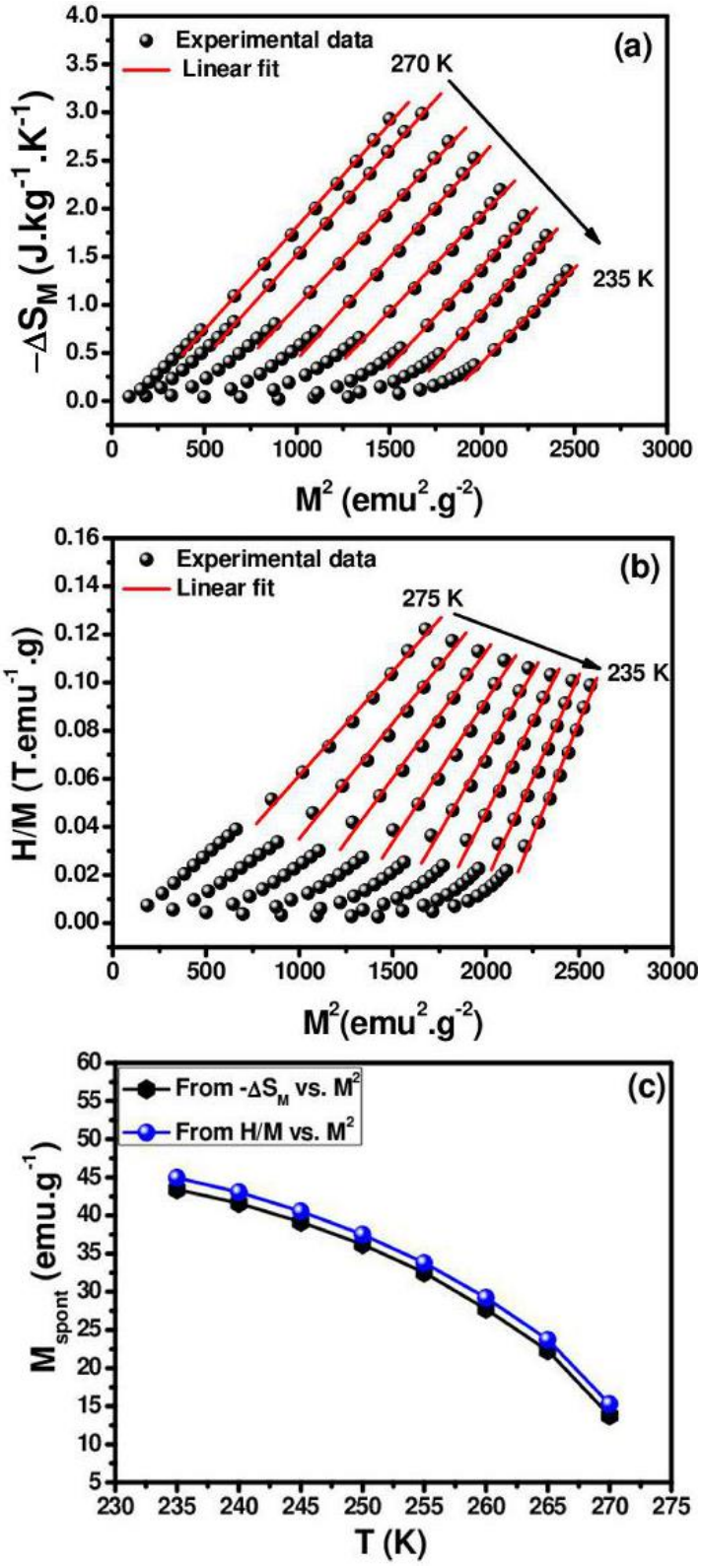

Fig. 8: (a) Linear fits (red lines) for $T < T_C$ of Arrott plots $\left(\frac{\mathrm{H}}{\mathrm{M}} vs.\mathrm{M}^2\right)$. **(b)** Linear fits (red lines) of $-\Delta S_M$ vs. M^2 curves. **(c)** M_{spont} vs. T deduced from $-\Delta S_M$ vs. M^2 curves (black symbols) and from the Arrott plots $\frac{\mathrm{H}}{\mathrm{M}}\ vs.\ \mathrm{M}^2$ (red symbols).

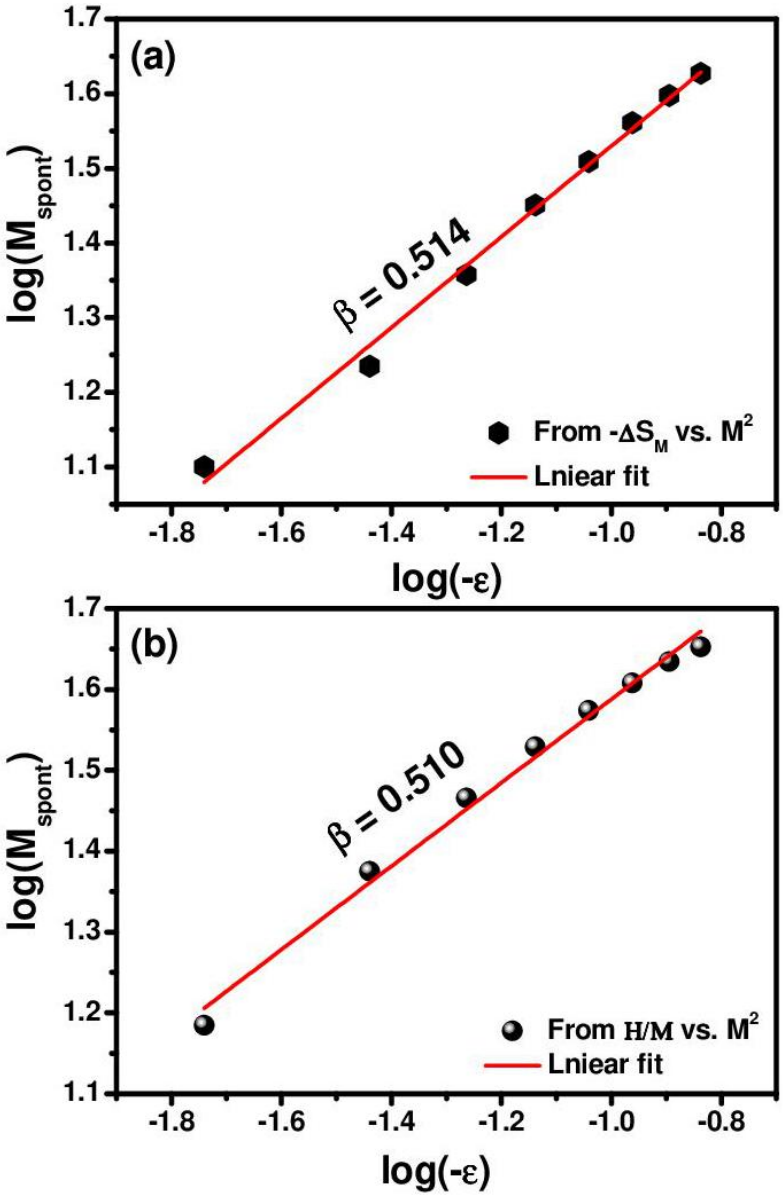

Fig. 9: Linear fit of $log\ M_{spont}\ \ vs.\ \ log\ (-\varepsilon)$ deduced from : **(a)** $-\Delta S_M$ vs. M^2 curves and **(b)** from the Arrott plots $\frac{\mathrm{H}}{\mathrm{M}}\ vs.\ \mathrm{M}^2$.